# A Comparative Study on the Evolution of Plastic Zone Between Indentation and Flattening Contact

Qingming Deng, Xiaochun Yin, and Magd Abdel Wahab

**Abstract** The peak of the ratio between the average pressure to yield strength is called hardness. The average contact pressure of elastic–plastic flattening and indentation contacts is studied by using numerical simulation. The similarity and difference between the two kinds of single asperity contacts are investigated. This paper chooses five kinds of elastic–plastic materials as the deformable-body. The yield strength of these materials covers the typical steel materials range used in the engineering project. And the effect of the evolution of the plastic zone under the contact surface on the contact pressure distribution is analyzed. Before the elastic zone under the contact surface disappears completely, the evolution of the plastic zone of the two types of contact is similar. However, the average pressure of indentation contact continues to increase after this, until it reaches the maximum. The average pressure of flattening contact reached the plateau since elastic core has disappeared, and after a while, it began to decrease.

**Keywords** Hardness · Flattening contact · Indentation contact · Average pressure · Finite element analysis

## 1 Introduction

Both flattening and indentation are fundamental problems in contact mechanics and have direct applications in a broad range of engineering fields [1–8]. Hertz [9] gave the prediction formulas for the pure elastic spherical contact. The Hertzian purely

Q. Deng (✉) · X. Yin
Department of Mechanics and Engineering Science, Nanjing University of Science and Technology, Nanjing 210094, China
e-mail: dqm2017@qq.com

X. Yin
e-mail: yinxiaochun2000@aliyun.com

Q. Deng · M. Abdel Wahab
Soete Laboratory, Department of Electrical Energy, Metals, Mechanical Constructions and Systems, Faculty of Engineering and Architecture, Ghent University, Ghent, Belgium

elastic contact theory [10] is shortly reviewed, here. The contact area and force of Hertz theory are given by:

$$A_E = \pi R' \omega \tag{1}$$

$$F_E = \frac{4}{3} \times E' \sqrt{R'} \times \omega^{\frac{3}{2}} \tag{2}$$

where $\omega$ is the interference between two contact bodies. And the equivalent elastic modulus, $E'$, and an equivalent radius, $R'$, are expressed as:

$$\frac{1}{E'} = \frac{1 - v_1^2}{E_1} + \frac{1 - v_2^2}{E_2} \tag{3}$$

$$\frac{1}{R'} = \frac{1}{R_1} + \frac{1}{R_2} \tag{4}$$

where $E_1$, $E_2$, $v_1$, $v_2$, $R_1$, and $R_2$ are Young's modulus, Poisson's ratio, and the radius of curvature of sphere and half-space, respectively. Later, many researchers have proposed many empirical models to predict contact response [9–17]. Ghaednia et al. divided those contact models into two categories: indentation and flattening model [11].

Figure 1 shows a schematic of a frictionless elastic–plastic half-space indented by a rigid sphere of radius R. The parameters $a$ and $a'$ are real contact radius and truncated contact radius, respectively. A normal force $F$ acts on top of a rigid sphere. The $\omega$ is interference between two contact bodies. Figure 2 shows a contact of an elastic–plastic hemisphere with a rigid half space. The hardness test is implemented to evaluate the material's resistance to plastic deformation. Indentation contact is an important research content about hardness test [11, 12]. The hardness $H$ is equal



**Fig. 1** An indentation model, in which the sphere is rigid and the flat is deformable
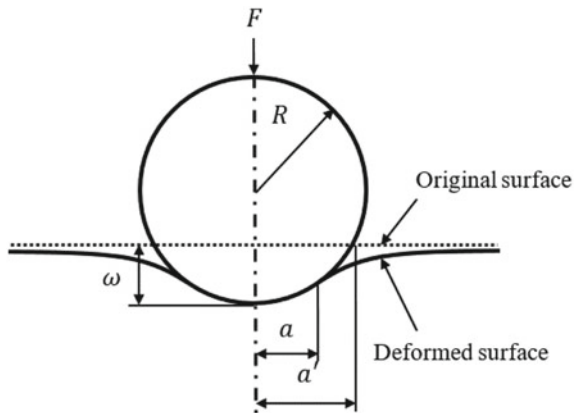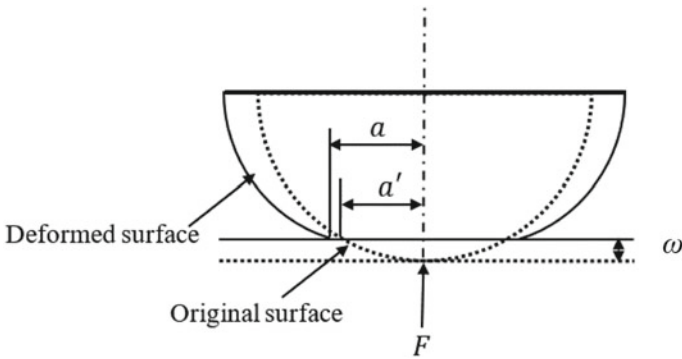
**Fig. 2** A flattening model, in which the flat is rigid and the sphere is deformable

to the average pressure when contact surface under fully plastic deformation. So the evolution of plastic zone under the contact surface is important for predict the hardness. Johnson [12] defined as $H = 2.8S_y$ using a constant multiple of yield strength. However, by using numerical simulation, Mesarovic and Fleck [13] found that the hardness depended on the material property. Other numerical research also had similar conclusions [11, 14–16].

And by observing the evolution of the plastic zone some new contact models were proposed [22–24]. The flattening contact is also a research hotspot. Many models suitable for flattening contact were proposed [17–21]. Kogut and Etsion also defined the hardness as a constant multiple of its yield strength ($H = 2.8S_y$). However, Jackson and Green found that the hardness of sphere was similar like half-space which depends on the material properties [14]. And they obtained a new critical interference $\omega_c$ resulting in the initial yield as:

$$\omega_c = \left( \frac{\pi \times c \times S_y}{2E'} \right)^2 R \tag{5}$$

where $S_y$ and $v$ are the yield limit and Poisson's ratio of the elastic–plastic body, respectively. And parameter $c$ is expressed as:

$$c = 1.295e^{0.736v} \tag{6}$$

Jackson and Kogut considered that the indentation contact had big difference compared with flattening contact [22]. However, when predicting hardness, there were cases where these two different contact models were mixed [14–16]. This abuse and mixing phenomenon also appeared in the prediction of collision problems [23]. The main purpose of this article is to compare the average pressure of two types of contact by studying the evolution of the plastic zone below the contact surface.

## 2   Finite Element Model

In this paper, for flattening and indentation contact problems, an axisymmetric 2-D model is used similar to other researches in the literature [14, 16, 18, 24–26]. The commercial program ANSYS™ is used. For indentation FEM model, as shown in Fig. 3a, the left side of the half-space is fixed horizontally and can move freely in the vertical direction. The bottom of half-space is completely fixed and a displacement $\omega$ is applied on the top of rigid sphere. The thickness $T$ and width $L$ are gradually increased, until the simulation result difference less than 1% between iterations as shown in Fig. 3. **Finite** element model of (a) indentation and (b) flattening contact, $L = 10R$ and $T = 6R$. For flattening model, the central axis of the hemisphere is fixed horizontally and is free vertically. The quadrilateral, eight node element solid183 is used here. The mesh size satisfies the study of convergence and the number of the elements under the contact surface should be more than 30 to ensure the accuracy of the contact radius.

For all cases, the elastic modulus and Poisson's ratio of deformable body are 200 GPa and 0.32, respectively. And yield strengths are 0.210, 0.5608, 0.9115, 1.2653, and 1.619 GPa. In the following, those five kinds of material models are referred to as Mat 1, Mat 2, Mat 3, Mat 4, and Mat 5. The deformation considered in this paper is before the contact radius reaches 0.8 $R$.
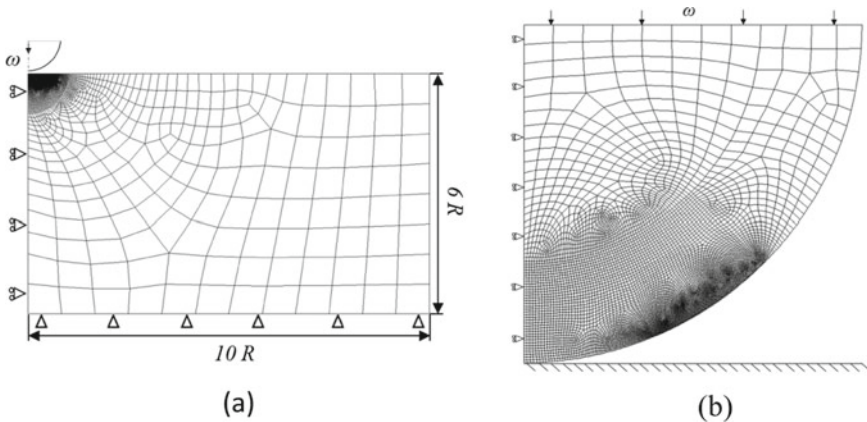


**Fig. 3**   Finite element model of **a** indentation and **b** flattening contact

**Fig. 4** Comparison of contact force predicted by simulation and Hertz theory in the elastic deformation regime
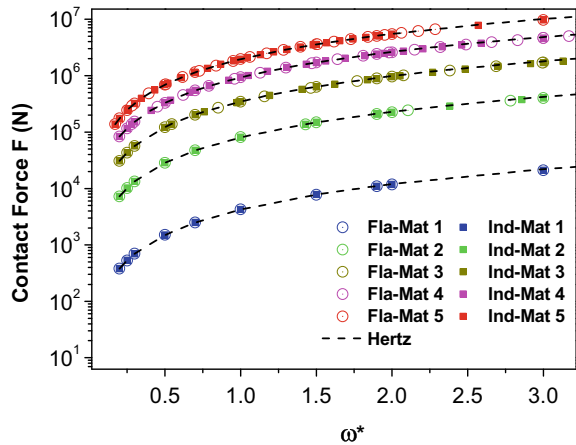


## 3 Numerical Results and Discussion

### 3.1 FEM Model Validation

Normally, the verification of the simulation model is verified by hertz theory. Figure 4 shows the comparison of contact force predicted by FEM and Hertz theory in the elastic phase. It shows that the maximum difference between FEM and Hertz results is less than 0.5%. This verifies the suitability of the finite element mesh shown in Fig. 3.

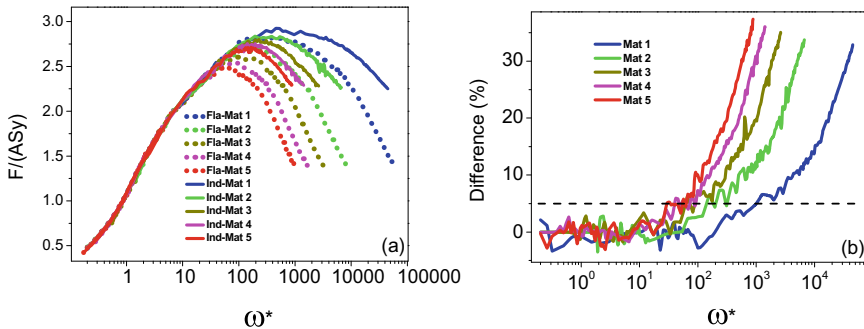### 3.2 The Ratio of Average Contact Pressure to Yield Strength

As interference increasing, the average contact pressure also increases. Until reaching a maximum, it will decrease with the increase of interference. This peak value is always considered to be the hardness of the material. Researchers use this to measure the ability of materials to resist plastic deformation.

The average contact pressure to yield strength ratio of all cases are shows in Fig. 5a. With the same deformable-body material, the two different contacts show similarity. It can be seen from Fig. 5b that when the deformation is small, the difference between the two types of contact is close to zero. Mat 5 case has larger similarity interference range than Mat 1 case.

In order to consider the different initial yield interference $\omega_c$ of different materials, the interference can be normalized through Eq. (5). And the variation of average contact pressure to yield strength ratio with dimensionless interference is shown in Fig. 6a. Compared with Fig. 5a, it can be seen that the different material cases have same change trend. As the interference increases, Mat 1 first plastically yields. In
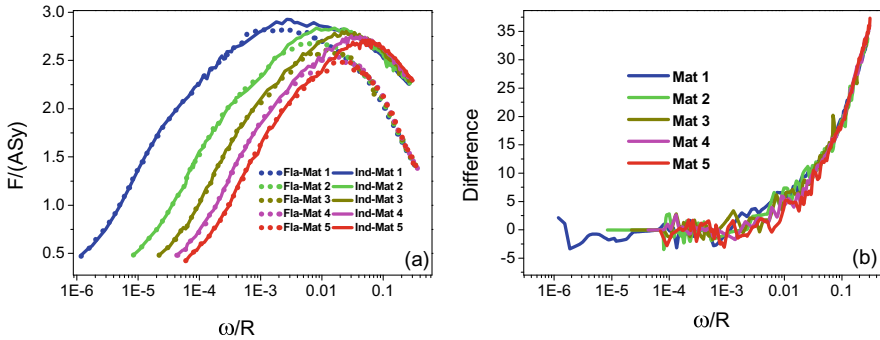
**Fig. 5**  **a** The variation of average contact pressure to yield strength ratio with interference. **b** The variation of difference with interference



**Fig. 6**  **a** The variation of average contact pressure to yield strength ratio with dimensionless interference and **b** The variation of difference with dimensionless interference

order to facilitate the evaluation of the difference between the two types of contact in engineering applications, the dimensionless interference that makes this difference reaches 5% is defined as the upper limit interference $\omega_{lh}^*$. When the dimensionless interference is less than $\omega_{lh}^*$, the average contact pressure difference is less than 5%, so the results are reliable when predicted with different contact models.

The $\omega_{lh}^*$ of different material cases predicted by the simulation are list in Table 1. And a prediction formula is given as:

**Table 1**  Upper limit interference for different material

| Material | Mat 1 | Mat 2 | Mat 3 | Mat 4 | Mat 5 |
|---|---|---|---|---|---|
| $E^*/S_y$ | 1061.03 | 397.32 | 244.45 | 176.1 | 137.626 |
| $\omega_{lh}^*$ | 1443.3 | 240.8158 | 116.0272 | 78.3215 | 57.6173 |

$$\omega_{lh}^* = 34.669 + 0.00141 \times \left(\frac{E^*}{S_y}\right)^{1.9827} \tag{7}$$
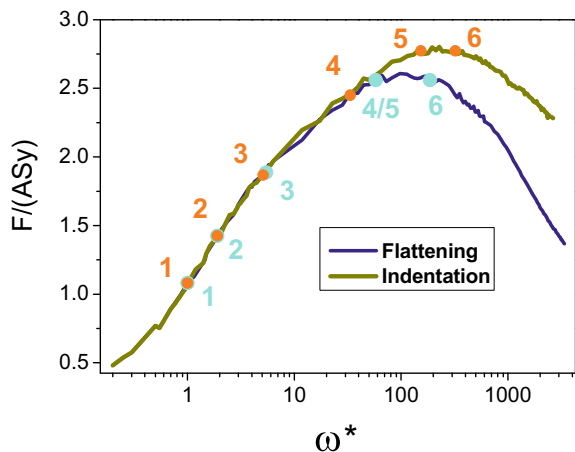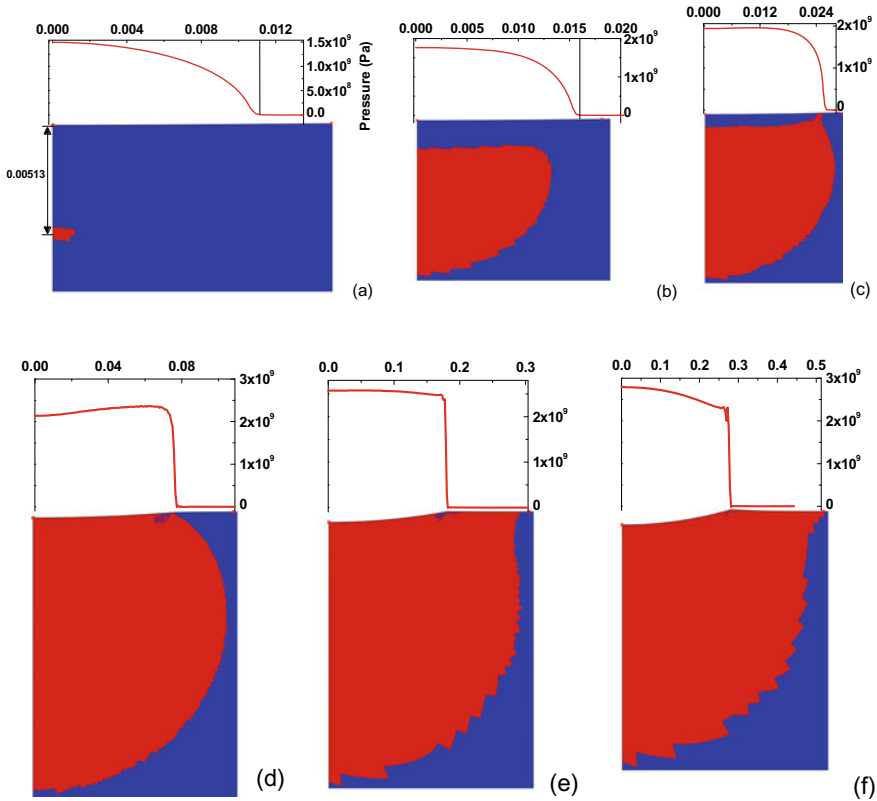
### 3.3 Plastic Zone Evolution

The change in contact response has a great relationship with the deformation near the contact surface. In order to study the effect of plastic zone evolution on average contact pressure, the indentation and flattening contact of Mat 3 are chosen as an example and are considered in this paper. According to the evolution characteristics of the plastic zone, the whole deformation process is divided into several stages as shown in Fig. 7. The plastic yield first appears ($\omega^* = 1$) as shown as point 1. And when $\omega^* = 1.9$, the plastic zone is in the subsurface of contact according to point 2. Plastic zone is for the first time reached and covers the whole surface according to point 3 and 4, respectively. During the deformation process, the average pressure will remain at the peak for a while, like a plateau as shown in Fig. 7 between point 5 and 6. It is worth noting that the flattening contact, point 4 coincides with point 5.

The plastic zone evolution of indentation and flattening contacts are shown in Figs. 8 and 9. As plotted in Figs. 8a and 9a, the initial plastic yield of both types of contact occurs when $\omega^* = 1$. And the initial yield point of indentation and flattening contact is located at $0.00513 R$ and $0.0052 R$ below the contact surface, respectively. The stress distribution on the contact surface complies with hertz theory.

And in the work of Jackson and Green [14], they considered that the dominance elastic contact phase will continue until $\omega^* = 1.9$ as shown in Figs. 8b and 9b. Although the plastic zone is large enough, the contact surface is still purely elastically deformed. Later on, the plastic zone will extend to the contact surface when $\omega^* =$

**Fig. 7** The average contact pressure to yield strength ratio of Mat 3

**Fig. 8** The plastic zone evolution of indentation contact

5.115 and $\omega^* = 5.44$ for indentation and flattening contact as shown in Figs. 8c and 9c. The stress distribution on the contact surface becomes flatter than elastic phase. At this stage, there is still a decreasing elastic core at the contact surface. The plastic zone, when this elastic core completely disappears ($\omega^* = 33.474$), and the two critical points of the average pressure plateau ($\omega^* = 153$ and $\omega^* = 321.317$) for indentation contact are shown in Fig. 8d–f. For flattening contact, when the elastic core disappear ($\omega^* = 57.7$), the average contact pressure will close to the peak value as shown in Fig. 9d. The distribution of the plastic zone when the average pressure starts to decrease ($\omega^* = 186.89$) is shown in Fig. 9e. It can be seen that before the elastic zone under the contact surface disappears completely, the evolution of the plastic zone of the two types of contact is very close. However, the average pressure of indentation contact continues to increase after this, until it reaches the maximum. The average pressure of flattening contact has reached the plateau since then, and after a while, it begins to decrease. So the maximum average pressure of the indentation contact is greater than the flattening contact.
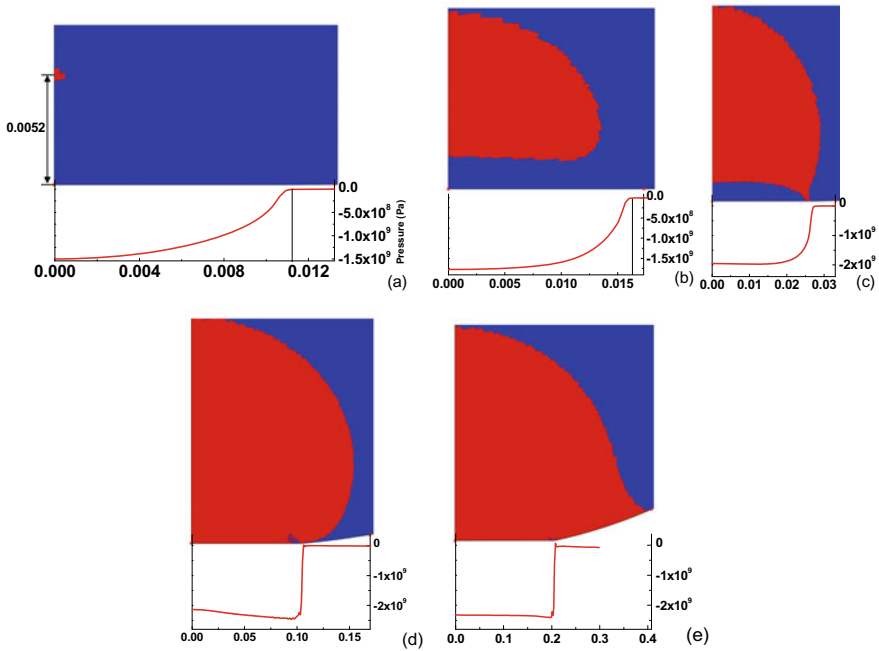
**Fig. 9** The plastic zone evolution of flattening contact

## 4 Conclusions

With the same deformable-body material cases, the average contact pressure of two different contacts show similarity. The larger yield strength case has a larger similarity interference range than the smaller cases. With dimensionless interference, smaller yield strength case has a larger similarity interference range than larger cases. And before the elastic zone under the contact surface disappears completely, the evolution of the plastic zone of the two types of contact is similar. However, the average pressure of indentation contact continues to increase after this, until it reaches the maximum. The average pressure of flattening contact has reached the plateau since elastic core disappear, and after a while, it begins to decrease. So the maximum average pressure of the indentation contact is greater than the flattening contact for the same deformation body cases.

# References

1. Mccarthy B et al (2002) A dynamic model, including contact bounce, of an electrostatically actuated microswitch. J Microelectromech Syst 11(3):276–283
2. Pal RK, Awasthi AP, Geubelle PH (2013) Wave propagation in elasto-plastic granular systems. Granular Matter 15(6):747–758
3. Komvopoulos K (2000) Head–disk interface contact mechanics for ultrahigh density magnetic recording. Wear 238(1):1–11
4. Cowles BA (1996) High cycle fatigue in aircraft gas turbines—an industry perspective. Int J Fract 80(2–3):147–163
5. Polycarpou AA, Etsion I (2000) A Model for the Static Sealing Performance of Compliant Metallic Gas Seals Including Surface Roughness and Rarefaction Effects. Tribol Trans 43(2):237–244
6. Wang Y et al (2002) A mixed-TEHD analysis and experiment of journal bearings under severe operating conditions. Tribol Int 35(6):395–407
7. Jiang X, Cheng HS, Hua DY (2000) A theoretical analysis of mixed lubrication by macro micro approach: part I—results in a gear surface contact. Tribol Trans 43(4):689–699
8. Kweh CC et al (1992) Simulation of elastohydrodynamic contacts between rough surfaces. J Tribol 114(3):412–419
9. Hertz H (1882) Ueber die Berührung fester elastischer Körper.: Journal für die reine und angewandte Mathematik (Crelle's Journal). Journal Für Die Reine Und Angewandte Mathematik
10. Hertz H (1882) Uber die beruhrung fester elastische korper und uber die harte (On the contact of rigid elastic solids and on hardness). Verhandlungen des Vereins zur Beforderung des Gewerbefleisses, Leipzig
11. Ghaednia H et al (2016) A comprehensive study of the elasto-plastic contact of a sphere and a flat. Tribol Int 93:78–90
12. Johnson KL (1987) Contact mechanics. Cambridge University Press
13. Mesarovic SD, Fleck NA (2000) Frictionless indentation of dissimilar elastic–plastic spheres. Int J Solids Struct 37(46–47):7071–7091
14. Jackson RL, Green I (2005) A finite element study of elasto-plastic hemispherical contact against a rigid flat. J Trib 127(2):343–354
15. Komvopoulos K, Ye N (2000) Three-dimensional contact analysis of elastic-plastic layered media with fractal surface topographies. J Trib 123(3):632–640
16. Song Z, Komvopoulos K (2013) Elastic–plastic spherical indentation: deformation regimes, evolution of plasticity, and hardening effect. Mech Mater 61:91–100
17. Chang W, Etsion I, Bogy DB (1987) An elastic-plastic model for the contact of rough surfaces. J Tribol 109(2):257–263
18. Kogut L, Etsion I (2002) Elastic-plastic contact analysis of a sphere and a rigid flat. J Appl Mech 69(5):657–662
19. Zhao Y, Maietta DM, Chang L (2000) An asperity microcontact model incorporating the transition from elastic deformation to fully plastic flow. J Trib 122(1):86–93
20. Jacq C et al (2002) Development of a three-dimensional semi-analytical elastic-plastic contact code. J Trib 124(4):653–667
21. Vu-Quoc L, Zhang X, Lesburg L (2000) A normal force-displacement model for contacting spheres accounting for plastic deformation: force-driven formulation. J Appl Mech 67(2):363–371
22. Jackson RL, Kogut L (2005) A comparison of flattening and indentation approaches for contact mechanics modeling of single asperity contacts. J Tribol 128(1):209–212
23. Wang H et al (2017) Experimental and theoretical analysis of the elastic-plastic normal repeated impacts of a sphere on a beam. Int J Solids Struct 109:131–142
24. Kogut L, Komvopoulos K (2004) Analysis of the spherical indentation cycle for elastic–perfectly plastic solids. J Mater Res 19(12):3641–3653

25. Larsson PL, Olsson E (2015) A numerical study of the mechanical behavior at contact between particles of dissimilar elastic–ideally plastic materials. J Phys Chem Solids 77:92–100
26. Olsson E, Larsson P-L (2016) A unified model for the contact behaviour between equal and dissimilar elastic–plastic spherical bodies. Int J Solids Struct 81:23–32